◆ Human Brain Mapping 36:3677–3686 (2015) ◆

Disrupted Brain Network Topology in Pediatric Posttraumatic Stress Disorder: A Resting-State fMRI Study

Xueling Suo,[1] Du Lei,[1] Kaiming Li,[1] Fuqin Chen,[2] Fei Li,[1] Lei Li,[1] Xiaoqi Huang,[1] Su Lui,[1] Lingjiang Li,[3] Graham J. Kemp,[4] and Qiyong Gong[1,5,6]*

[1]Huaxi MR Research Center (HMRRC), Department of Radiology, West China Hospital of Sichuan University, Chengdu, Sichuan, China
[2]Department of Medical Information Engineering, School of Electrical Engineering and Information, Sichuan University, Chengdu, Sichuan, China
[3]Mental Health Institute, the Second Xiangya Hospital of Central South University, Changsha, Hunan, China
[4]Department of Musculoskeletal Biology and MRC-Arthritis Research UK Centre for Integrated Research into Musculoskeletal Ageing (CIMA), Faculty of Health and Life Sciences, Magnetic Resonance and Image Analysis Research Centre (MARIARC) and Institute of Ageing and Chronic Disease, University of Liverpool, Liverpool, United Kingdom
[5]Department of Psychology School of Public Administration, Sichuan University, Chengdu, Sichuan, China
[6]Department of Psychiatry, West China Hospital of Sichuan University, Chengdu, Sichuan, China

Abstract: Children exposed to natural disasters are vulnerable to the development of posttraumatic stress disorder (PTSD). Recent studies of other neuropsychiatric disorders have used graph-based theoretical analysis to investigate the topological properties of the functional brain connectome. However, little is known about this connectome in pediatric PTSD. Twenty-eight pediatric PTSD patients and 26 trauma-exposed non-PTSD patients were recruited from 4,200 screened subjects after the 2008 Sichuan earthquake to undergo a resting-state functional magnetic resonance imaging scan. Functional connectivity between 90 brain regions from the automated anatomical labeling atlas was established using partial correlation coefficients, and the whole-brain functional connectome was constructed by applying a threshold to the resultant 90 * 90 partial correlation matrix. Graph theory analysis was then used to examine the group-specific topological properties of the two functional connectomes. Both the PTSD and non-PTSD control groups exhibited "small-world" brain network topology. However, the functional connectome of the PTSD group showed a significant increase in the clustering coefficient and a normalized characteristic path length and local efficiency, suggesting a shift toward regular networks.

Xueling Suo and Du Lei contributed to this work equally.

Contract grant sponsor: National Natural Science Foundation; Contract grant numbers: 81030027, 81227002 and 81220108013; Contract grant sponsor: National Key Technologies R&D Program of China; Contract grant numbers: 2012BAI01B03; Contract grant sponsors: Program for Changjiang Scholars and Innovative Research Team in University of China; Contract grant numbers: IRT1272 and T2014190; Contract grant sponsors: China Postdoctoral Science Foundation; Contract grant numbers: 2012M521696 and 2013T60856

*Correspondence to: Qiyong Gong; Professor of Radiology, Psychology and Psychiatry, Huaxi MR Research Center (HMRRC), Department of Radiology, West China Hospital of Sichuan University, No. 37 Guo Xue Xiang, Chengdu, Sichuan 610041, China. E-mail: qiyonggong@hmrrc.org.cn

Received for publication 25 December 2014; Revised 26 March 2015; Accepted 27 May 2015.

DOI: 10.1002/hbm.22871

Published online 19 June 2015 in Wiley Online Library (wileyonlinelibrary.com).

© 2015 Wiley Periodicals, Inc.

Furthermore, the PTSD connectomes showed both enhanced nodal centralities, mainly in the default mode- and salience-related regions, and reduced nodal centralities, mainly in the central-executive network regions. The clustering coefficient and nodal efficiency of the left superior frontal gyrus were positively correlated with the Clinician-Administered PTSD Scale. These disrupted topological properties of the functional connectome help to clarify the pathogenesis of pediatric PTSD and could be potential biomarkers of brain abnormalities. *Hum Brain Mapp 36:3677–3686, 2015.* © 2015 Wiley Periodicals, Inc.

Key words: pediatric PTSD; r-fMRI; graph theory; functional connectome; small-worldness

INTRODUCTION

Childhood and adolescence are crucial stages of physical and psychological development. Catastrophic experiences, such as the 2008 Sichuan 8.0 magnitude earthquake, can lead to psychological and behavioral problems, including mental disorders. Posttraumatic stress disorder (PTSD) can cause lifelong suffering. Pediatric PTSD is not uncommon, the prevalence among children (12–17 years) being 3.7% for boys and 6.3% for girls [Kilpatrick et al., 2003], and its pathogenesis remains largely unknown.

Previous brain magnetic resonance (MR) studies in pediatric PTSD have focused mainly on structural changes, finding these changes in corpus callosum [De Bellis et al., 1999, 2002b; De Bellis and Keshavan, 2003; Jackowski et al., 2008; Teicher et al., 2004], prefrontal cortex [Carrion et al., 2009; De Bellis et al., 2002b; Richert et al., 2006], and temporal lobe [De Bellis et al., 1999, 2002b]. There have been few functional neuroimaging studies. Carrion et al. found that young people who had experienced interpersonal trauma and who exhibited posttraumatic stress symptoms showed increased activation in the medial prefrontal cortex and decreased activation in dorsolateral prefrontal cortex (dlPFC) during response inhibition tasks [Carrion et al., 2008]. Yang et al. found that viewing earthquake imagery, adolescents with PTSD showed activation in the bilateral visual cortex, bilateral cerebellum, and left parahippocampal gyrus [Yang et al., 2004]. However, little is known about the functional brain changes in PTSD under resting-state conditions.

The human brain is a complex network, and recent advances in graph-based theoretical approaches have allowed for noninvasive characterization of its topological properties, which proves to be a very effective and informative way to explore brain function and human behavior [Bullmore and Bassett, 2011; Bullmore and Sporns, 2009]. In graph theory, a network is represented as nodes that are connected by edges. A node is a brain region, and an edge is present when there is an anatomical connection or functional correlation between two nodes. Simple examples of network topologies are regular and random networks. Regular networks are characterized by high clustering (the probability that neighboring nodes are interconnected with other neighboring nodes as well) and a long average path length (the average distance from one node to any other node in the network, expressed as the number of links that must be traveled). In contrast, random networks have low clustering and a short average path length, in which nodes are randomly connected to each other. Watts and Strogatz first proposed a mathematical model called the "small-world" network, corresponding to an intermediate state between regular and random networks. Small-world networks were quantitatively described as having a high degree of clustering and a short path length between brain regions [Watts and Strogatz, 1998], enabling the specialization and integration of complex networks at a low "wiring cost" [Achard and Bullmore, 2007; Sporns and Zwi, 2004]. Studies have revealed this small-world organization in the large-scale structural [He et al., 2007] and functional [Bassett et al., 2006] brain connectome. Furthermore, abnormal small-world properties have been found in neuropsychiatric disorders, including Alzheimer's disease [Supekar et al., 2008], schizophrenia [Liu et al., 2008], epilepsy [Liao et al., 2010], and depression [Zhang et al., 2011]. Although different brain diseases show different changes, the topology of the functional network of an abnormal brain can be regarded as less optimal the more it deviates from small-world network topology, suggesting both a possible role in pathophysiology and potential use as a biomarker. In adult PTSD, a diffusion tensor imaging (DTI) study showed the loss of small-world characteristics in structural brain networks [Long et al., 2013]. However, the topological characteristics of the functional connectomes in pediatric PTSD are largely unknown. Because children are particularly vulnerable to the development of PTSD after trauma, we hypothesized that the small-world properties of functional connectomes would be abnormal in pediatric PTSD.

To test our hypothesis, we used resting-state functional magnetic imaging (r-fMRI) to construct the brain functional connectomes of both pediatric PTSD patients and trauma-exposed non-PTSD controls. We applied graph-based theoretical approaches to define and compare the topological properties of reconstructed functional connectomes in both groups and to investigate possible relationships with clinical variables.

MATERIALS AND METHODS

Participants

The subjects were recruited in the town of Hanwang and in Beichuan County 8–15 months after the 8.0 magnitude earthquake that occurred in Sichuan in May 2008. A

total of 4,200 earthquake survivors were screened between January and August 2009, using four inclusion criteria: (i) personal experience of the earthquake; (ii) personal witnessing of death, serious injury, or the collapse of buildings; (iii) age < 18 years old; and (iv) IQ > 80. Each participant was interviewed and screened using the PTSD checklist (PCL) [Weathers et al., 1994]; those participants who scored >35 on the PCL were administered the Clinician-Administered PTSD Scale (CAPS) [Blake et al., 1995] by an experienced psychiatrist (Lingjiang Li, 30 years' experience), and those who scored >50 on the CAPS were diagnosed with PTSD; those who scored <30 on PCL were considered as non-PTSD controls [Jin et al., 2014] and were not assessed using the CAPS. This process identified 161 PTSD patients and 99 trauma-exposed non-PTSD controls with similar demographic characteristics, lifestyles, and earthquake experiences. The exclusion criteria for all of the subjects included psychiatric comorbidities assessed using the structured clinical interview for the diagnostic and statistical manual of mental disorders, fourth edition (DSM-IV) [First et al., 2002], a history of psychiatric or neurological disorders ($n = 42$), magnetic resonance imaging (MRI) contraindications ($n = 30$), recent medication that might affect brain function ($n = 24$), unavailability of key data ($n = 12$), left-handedness ($n = 10$), a CAPS score > 35 but <50 ($n = 8$) [Jin et al., 2014], and a history of or current brain injury ($n = 7$). This process yielded 28 drug-naive, first-episode PTSD patients, and 26 trauma-exposed non-PTSD controls who underwent MR scanning, data from four PTSD patients and two controls being excluded later because of excessive movement (translational movement > 3.0 mm and/or rotation > 3.0°). The MR data from 24 PTSD patients and 24 controls went forward for analysis. The demographic and clinical characteristics of these subjects are summarized in Table I.

This study was approved by the Research Ethics Committee of the West China Hospital of Sichuan University. Each child's guardian was provided with a detailed information sheet about the study and then provided written consent.

TABLE I. Demographics and clinical characteristics of the subjects[a]

Variables	PTSD ($n = 24$)	Non-PTSD ($n = 24$)	P value
Age (years)[b]	13.0 ± 1.8 (10–16)	13.0 ± 1.4 (11–16)	0.28[c]
Gender (male/female)	9/15	10/14	0.15[d]
Handedness (right/left)	24/0	24/0	–
Years of education[b]	8.0 ± 2.3 (6–12)	8.0 ± 2.2 (6–14)	0.71[c]
Time since trauma (months)[b]	10.3 ± 1.6 (8–13)	13.3 ± 1.4 (10–15)	0.19[c]
PCL	54.6 ± 4.8 (40–65)	23.7 ± 3.0 (19–35)	–
CAPS	65.5 ± 6.4 (60–86)	–	–

[a]Data are presented as the mean ± SD (range of minimum–maximum).
[b]Age, years of education and time since trauma were reported by participants' parents/guardians at the time of magnetic resonance scanning.
[c]P value obtained by two-tailed two-sample t test.
[d]P value obtained by two-tailed Pearson chi-square test.
Abbreviation: PTSD, post traumatic stress disorder; PCL, PTSD checklist; CAPS, Clinician-administered PTSD scale.

r-fMRI Data Acquisition and Preprocessing

A r-fMRI dataset was acquired using a 3-T magnetic resonance system (GE EXCITE, Milwaukee, WI) with an eight-channel phased array head coil. The participants were instructed to keep their eyes closed and to think of nothing in particular during the acquisition. The sequence parameters were repetition time/echo time (TR/TE) 2000/30 ms; flip angle 90°; 30 axial slices per volume; 5 mm slice thickness (no slice gap); matrix 64 × 64; field of view (FOV) 240 × 240 mm^2; voxel size 3.75 × 3.75 × 5 mm^3. A total of 200 volumes were collected for each subject. All of the MR images were evaluated for clinical abnormalities by a neuroradiologist (Su Lui, 10 years of experience).

Image preprocessing was performed using SPM8 (http://www.fil.ion.ucl.ac.uk/spm). The first 10 time points were discarded to avoid instability of the initial MRI signal. After correction for intravolume acquisition time delay and head motion, the images were spatially normalized to a 3 × 3 × 3 mm^3 Montreal Neurological Institute 152 template and then linearly detrended and temporally bandpass filtered (0.01–0.08 Hz) to remove low-frequency drift and high-frequency physiological noise. Finally, the global signal, the white matter signal, the cerebrospinal fluid signal, and the motion parameters (three translational and three rotational parameters) were regressed out (Fox et al., 2009).

Functional Connectivity Matrix and Graph Construction

The network was constructed using GRETNA (http://www.nitrc.org/projects/gretna/) [He et al., 2008; Zhang et al., 2011]. First, the automated anatomical labeling (AAL) atlas [Tzourio-Mazoyer et al., 2002] was used to divide the whole brain into 90 cortical and subcortical regions of interest, and each was considered a network node. Next, the mean time series was acquired for each region, and the partial correlations of the mean time series between all pairs of nodes (representing their conditional dependences by excluding the effects of the other 88 regions) were considered the edges of the network [Jin et al., 2011; Tao et al., 2013; Zhang et al., 2011]. This process resulted in a 90 × 90 partial correlation matrix for each subject, which was converted into a binary matrix (i.e., adjacency matrix) according to a predefined threshold (see below for the threshold selection), where the entry $a_{ij} = 1$ if the absolute partial correlation between regions i and j exceeds threshold and $a_{ij} = 0$ otherwise [Zhang et al., 2011].

The networks of individual subjects differed in the number of edges [Wen et al., 2011]. To address this difference, we applied a range of sparsity thresholds, S, to the correlation matrices to provide each graph with the same number of edges. For each subject, S was defined as the fraction of the total number of edges remaining in a network; its minimum was set so that the averaged node degree of the thresholded network was $2\log(N)$, where N is the number of nodes [Zhang et al., 2011], and its maximum so that the small-worldness scalar σ of the thresholded network was >1.1. This procedure generated a threshold range of $0.10 < S < 0.34$ with an interval of 0.01. This threshholding strategy [Zhang et al., 2011] produced networks that could estimate small-worldness with sparse properties and the minimum possible number of spurious edges [Watts and Strogatz, 1998; Zhang et al., 2011]. For the brain networks at each sparsity level, we calculated both global and node network metrics.

Small-World Properties and Network Efficiency

The global metrics examined included small-world parameters (for definitions see [Watts and Strogatz, 1998]), including the clustering coefficient C_P, characteristic path length L_P, normalized clustering coefficient γ, normalized characteristic path length λ, and small-worldness σ, as well as network efficiency parameters (for definitions see [Latora and Marchiori, 2001]), including the local efficiency E_{loc} and global efficiency E_{glob}. We calculated L_p as the harmonic mean distance between all possible pairs of regions to address the disconnected graphs dilemma [Newman, 2003]. The node metrics examined included the node degree, efficiency, and betweenness centrality.

Statistical Analysis

We calculated the area under the curve (AUC) for each network metric. The AUC for a general metric Y was calculated over the sparsity range from S_1 to S_n with an interval of ΔS, here $S_1 = 0.10$, $S_n = 0.34$, and $\Delta S = 0.01$. The AUC provided a summarized scalar for the topological characterization of brain networks, that is, independent of a single threshold selection and sensitive to topological alterations in brain disorders [Wang, et al., 2009a; Zhang, et al., 2011].

To locate the specific pairs of brain regions with altered functional connectivity in PTSD patients, we identified region pairs that exhibited between-group differences in nodal characteristics and then used the network-based statistics (NBS) method (http://www.nitrc.org/projects/nbs/) [Zalesky et al., 2010] to locate the connected regions showing significant changes [Li et al., 2013; Zalesky et al., 2011; Zhang et al., 2011]. Specifically, for each subject, we chose the nodes that exhibited significant between-group differences in at least one of the three nodal centralities (node degree, efficiency, and betweenness), we generated a subset of the connections matrix and then applied the NBS method to define a set of suprathreshold links among any connected components (threshold, $T = 2.0$, $P < 0.05$). The significance for each was estimated using the nonparametric permutation method (10,000 permutations). For a detailed description see Zalesky et al. [2010].

Using Matlab (www.mathworks.com), we applied nonparametric permutation tests [Zhang et al., 2011] to identify significant between-group differences in the AUCs of all of the network metrics, to compare the small-world properties, network efficiency, and nodal characteristics of the functional connectomes between the PTSD patients and the non-PTSD controls. Briefly, we first calculated the between-group difference in the mean value of each network metric. To test the null hypothesis, we randomly reallocated all of the values for each network metric into two groups and recomputed the mean differences between them. This randomization procedure was repeated 10,000 times, and the 95th percentile points of each distribution were used as the critical values for a two-tailed test of the null hypothesis with a type I error of 0.05. To address the problem of multiple comparisons, we adopted a Benjamini Hochberg false discovery rate (FDR) correction method at a significance level of 0.05 [Benjamini et al., 2001].

After significant between-group differences had been identified in the network metrics, we correlated these metrics with the CAPS scores in the PTSD group, using age, and gender as covariates.

The statistical analysis of the demographic and clinical data was performed with SPSS software (http://www.spss.com), version 16.0 (Chicago, IL).

RESULTS

Demographic and Clinical Comparisons

There were no significant differences in age, gender, education, or time as the trauma between the PTSD patients and the trauma-exposed non-PTSD controls ($P > 0.05$; Table I).

Global Topological Organization of the Functional Connectome

In the defined threshold range, both the pediatric PTSD group and the non-PTSD control group showed small-world topology in the brain functional connectome (Fig. 1). The PTSD group, compared with the non-PTSD subjects, showed a significantly increased clustering coefficient C_p ($P = 0.0056$) and normalized characteristic path length λ ($P = 0.0298$), with no significant differences in γ ($P = 0.2559$), L_p ($P = 0.1158$), or σ ($P = 0.1648$). With regard to network efficiency, the PTSD group showed a significantly increased E_{local} ($P = 0.0190$) (Fig. 2), with no significant difference in E_{global} ($P = 0.0868$).

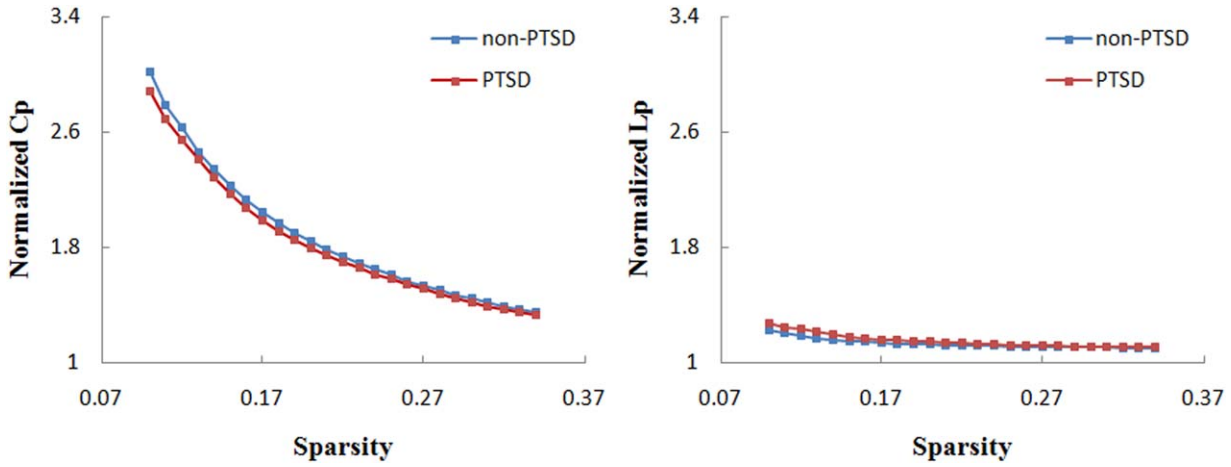

Figure 1.

The key small-world parameters of the functional connectome as a function of sparsity threshold. Both the PTSD group and the trauma-exposed non-PTSD group showed a normalized C_p greater than 1 and a normalized L_p approximately equal to 1, indicating that both groups exhibited a small-world topology. PTSD: post traumatic stress disorder; C_p: clustering coefficient; L_p: characteristic path length.

Regional Topological Organization of the Functional Connectome

We identified the brain regions showing significant between-group differences in at least one nodal metric ($P < 0.05$, uncorrected). Compared with the non-PTSD controls, the PTSD patients showed increased nodal centralities in the left superior frontal gyrus (SFG), left gyrus rectus (REC), left superior temporal gyrus (STG), right middle temporal gyrus (MTG), bilateral thalamus, and bilateral middle occipital gyrus (MOG). Decreased nodal centralities were found in the right dlPFC (right middle frontal gyrus, right inferior frontal gyrus), bilateral inferior parietal gyrus (IPG), and left lingual gyrus (LG) (Fig. 3A, Table II).

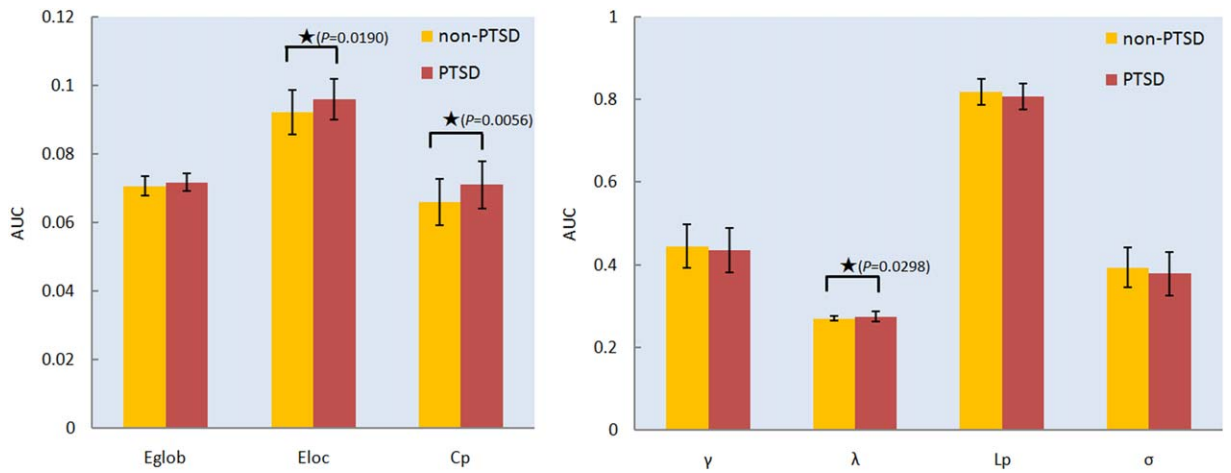

Figure 2.

The differences in topological properties of the brain functional connectome between pediatric PTSD and trauma-exposed non-PTSD patients. Significant differences were found in C_p ($P = 0.0056$), λ ($P = 0.0298$) and E_{local} ($P = 0.0190$) in pediatric PTSD patients. The black stars (★) indicate statistically significant differences between the two groups ($P < 0.05$, uncorrected). Error bars denote standard deviations. PTSD: posttraumatic stress disorder; E_{global}: global efficiency; E_{local}: local efficiency; C_p: clustering coefficient; γ: normalized clustering coefficient; λ: normalized characteristic path length; L_p: characteristic path length; σ: small-worldness; AUC: area under the curve.

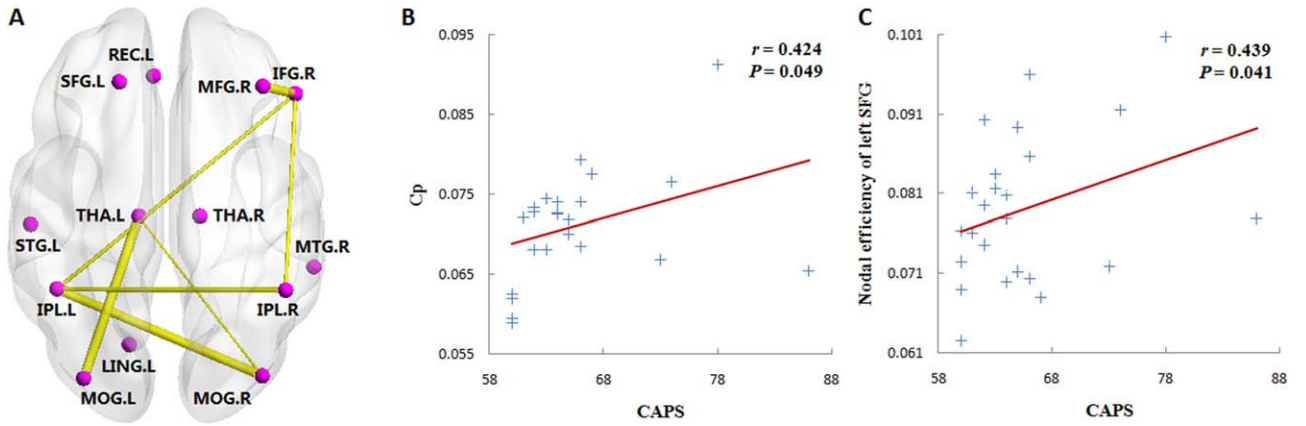

Figure 3.

(A) Significantly altered nodal centralities of the brain functional connectome in pediatric PTSD patients, compared with trauma-exposed non-PTSD controls ($P < 0.05$, uncorrected). All connections exhibited decreased values in the PTSD patients. These connections formed a single connected network with 13 nodes and seven connections ($P = 0.007$, corrected). The results were visualized using the BrainNet viewer package (http://www.nitrc.org/projects/bnv). (**B**, **C**) Scatter plots of C_p and the nodal efficiency of the left SFG compared to CAPS scores. PTSD: posttraumatic stress disorder; CAPS: Clinician-Administered PTSD Scale; C_p: clustering coefficient; L: left; R: right; SFG: superior frontal gyrus; MFG: middle frontal gyrus; IFG: inferior frontal gyrus; REC: rectus gyrus; THA: thalamus; STG: superior temporal gyrus; MTG: middle temporal gyrus; IPL: inferior parietal lobe; MOG: middle occipital gyrus; LING: lingual gyrus.

PTSD-Related Alterations in Functional Connectivity

The NBS method identified a significantly altered network in the PTSD patients. This network had 13 nodes and seven connections (Fig. 3A, Table III), and the nodes included several central executive regions (e.g., dlPFC and parietal regions), occipital regions, and the thalamus. Within this network, all of the connections were decreased in the PTSD patients compared with non-PTSD controls.

Relationships Between Network Metrics and Clinical Variables

CAPS score was positively correlated with C_p ($P = 0.049$; Fig. 3B) but not with the other global metrics: L_p ($P = 0.872$), γ ($P = 0.257$), σ ($P = 0.170$), E_{loc} ($P = 0.129$), or E_{glob} ($P = 0.553$). CAPS score was also positively correlated with the nodal efficiency of the left SFG ($P = 0.041$; Fig. 3C) but not with the other nodal metrics.

DISCUSSION

We applied graph-based theoretical approaches to analyze the brain functional connectome topology in pediatric patients with PTSD compared with trauma-exposed non-PTSD controls. There were three main findings: (1) at the global level, the PTSD patients had altered small-worldness in the functional connectome, that is, a shift toward a regular organization; (2) at the nodal level, the PTSD patients showed: (a) increased nodal characteristics in the default-mode regions, bilateral thalamus and MOG; and (b) reduced nodal centralities in the central executive

TABLE II. Regions showing altered nodal centralities in the pediatric PTSD group when compared with the trauma-exposed non-PTSD control group

	P values		
Brain regions	Nodal degree	Nodal efficiency	Nodal betweenness
PTSD > Non-PTSD			
Left superior frontal gyrus	**0.0470**	**0.0076**	**0.0096**
Left gyrus rectus	0.2102	0.3575	**0.0020**
Left middle occipital gyrus	**0.0114**	**0.0112**	0.5101
Right middle occipital gyrus	**0.0188**	**0.0186**	0.3247
Left thalamus	**0.0374**	**0.0274**	0.3743
Right thalamus	**0.0488**	**0.0286**	0.1444
Left superior temporal gyrus	0.0628	0.0586	**0.0476**
Right middle temporal gyrus	**0.0216**	**0.0190**	**0.0180**
PTSD < Non-PTSD			
Right middle frontal gyrus	**0.0234**	**0.0500**	0.2597
Right inferior frontal gyrus	**0.0104**	**0.0376**	0.0728
Left lingual gyrus	0.4903	0.4529	**0.0328**
Left inferior parietal gyrus	**0.0140**	0.0674	0.0990
Right inferior parietal gyrus	**0.0420**	0.1000	0.4155

Regions were considered abnormal in the pediatric PTSD patients if they exhibited significant between-group differences ($P < 0.05$, uncorrected) in at least one of the three nodal centralities (shown in bold font).
Abbreviation: PTSD, posttraumatic stress disorder.

TABLE III. Decreased functional connections in the pediatric PTSD group compared with the trauma-exposed non-PTSD control group

Region 1	Category	Region 2	Category	*t*-score	Interlobe
Left middle occipital gyrus	Occipital	Left thalamus	Subcortical	2.69	Yes
Right middle frontal gyrus	Frontal	Right inferior frontal gyrus	Frontal	2.64	No
Right middle occipital gyrus	Occipital	Left inferior parietal gyrus	Parietal	2.64	Yes
Left inferior parietal gyrus	Parietal	Right inferior parietal gyrus	Parietal	2.30	No
Right inferior frontal gyrus	Frontal	Left inferior parietal gyrus	Parietal	2.20	Yes
Right inferior frontal gyrus	Frontal	Right inferior parietal gyrus	Parietal	2.19	Yes
Right middle occipital gyrus	Occipital	Left thalamus	Subcortical	2.08	Yes

Connections are listed in descending order of statistical significance ($P < 0.05$). These connections formed a connected network identified using a network-based statistic approach ($P = 0.007$, corrected). See Figure 3A for a graphical presentation of these connections.
Abbreviation: PTSD, posttraumatic stress disorder.

regions and left LG; and (3) the C_p and the nodal efficiency of the left SFG positively was correlated with the CAPS score. These results provided unequivocal evidence of a topological alteration of the functional connectome in pediatric PTSD. We suggest below some possible pathophysiological implications.

In accordance with their finding of increased global integration and maintained local clustering, the authors of a previous DTI tractography study speculated that the adult PTSD group showed a shift toward a randomized configuration [Long et al., 2013]. This randomization process (in which the network transforms from a small-world to a more random network) has been considered a general pattern of several neuropsychiatric diseases such as schizophrenia [Lynall et al., 2010] and major depression disorder [Zhang et al., 2011]. Unlike in previous adult PTSD studies, we identified a higher clustering coefficient and normalized characteristic path length in pediatric PTSD, which are typical features of regular organization, which has been considered another general pattern of several neuropsychiatric diseases such as attention-deficit/hyperactivity disorder [Wang et al., 2009b] and temporal lobe epilepsy [Bernhardt et al., 2011]. It is possible that differences in subjects and modalities of connectivity measurement account for this difference. However, the clustering coefficient C_p was positively correlated with the CAPS score in our pediatric PTSD patients (Fig. 3B), indicating a shift to a more regular organization in the functional connectome. Although the biology underlying the shift remains unclear, this regularization process (in which the network transforms from a small-world to a more regular network) is generally associated with reduced signal propagation speed and synchronizability [Strogatz, 2001]. At the microscopic level, neuronal connectivity is influenced by neuronal activity, gene expression, hormones, and signaling of supporting cells such as astrocytes [Joseph D'Ercole and Ye, 2008; Rose et al., 2004; Sahara and O'Leary, 2009]. The psychobiological data suggest that children and adolescents with abuse-related PTSD have altered catecholamines and hypothalamic–pituitary–adrenal (HPA) axis activity [De Bellis et al., 2002b]. In the developing brain, elevated levels of catecholamines and cortisol can lead to adverse brain development through the mechanisms of accelerated loss (or metabolism) of neurons [Simantov et al., 1996], delays in myelination [Dunlop et al., 1997], abnormalities in developmentally appropriate pruning [Todd, 1992], and inhibition of neurogenesis [Tanapat et al., 1998]. Thus, we speculate that the PTSD-related network shift abnormalities we have observed might be related to altered catecholamines and HPA axis activity. We also identified higher local efficiency, indicative of compensatory mechanisms that form clusters to preserve efficient communication [Caeyenberghs et al., 2012].

In addition to the global topologies, we also studied the node attributes of the brain connectome. These nodal characteristics reflect the roles of nodes in information transport and integration across the network [Sporns et al., 2007], and so altered nodal characteristics indicate abnormalities in relevant brain region activation. The main increased nodal activities we observed were within the default mode network (DMN), which has been linked to various processes of internal mentation [Andrews-Hanna, 2012]. Specifically, the increased nodal centralities in the left SFG, left REC, left STG, and right MTG we identified might be related to altered processing of negative emotions [Yin et al., 2012], self-relatedness [Liberzon and Sripada, 2008], hyperarousal [De Bellis et al., 2002a], and abnormal memory retrieval [Buckner et al., 2008]. Furthermore, the increased nodal efficiency of the left SFG was positively correlated with the CAPS score in the pediatric PTSD patients (Fig. 3C). Previous structural studies have demonstrated that PTSD patients have reduced gray matter volume of the left SFG, associated with hyperarousal [Weber et al., 2013]. Neuroimaging studies have also found greater activation in the SFG in PTSD [Lanius et al., 2004; Lindauer et al., 2008; Whalley et al., 2009]. Thus, we speculate that the left SFG neural metrics might be associated with the severity of PTSD. Together, the increased nodal centralities of the DMN regions suggest their strengthened roles in coordinating whole-brain networks, presumably in response to the pathological disorder of PTSD. We also found increased nodal centralities in the

bilateral thalamus, which are components of the salience network (SN) responsible for detecting and responding to salient stimuli [Seeley et al., 2007]; the thalamus is a "sensory gate" that relays sensory information to different parts of the cerebral cortex [Lanius et al., 2003]. The thalamus has been implicated in PTSD [Felmingham et al., 2008; Kim et al., 2007]. For instance, increased activation was found in the thalami of PTSD patients during the recall of a neutral memory [Lanius et al., 2004]; conceivably, abnormal nodal centralities of the bilateral thalamus might be involved in the disruption of emotional processing in PTSD patients.

The decreased nodal centralities we observed were mainly in the central executive network (CEN), including the right dlPFC and bilateral IPG. The CEN has been associated with processes related to goal-directed behaviors, working memory, and attention control [Menon, 2011], and it is reportedly impaired in PTSD [Weber et al., 2005]. It has recently been proposed that the functional alterations of PTSD involve a triple network model, which largely overlaps with the DMN, SN, and CEN [Menon, 2011; Patel et al., 2012]. The SN controls the interaction between the DMN and CEN [Sridharan et al., 2008]. Our findings are supported by a working memory study in which the control group showed stronger connectivity in the SN and CEN [Daniels et al., 2010]. Our NBS results also provided support for this (Fig. 3A). However, the relationships of the SN, DMN, and CEN in PTSD have not been studied in detail, and the evidence has been conflicting: for example, Sripada et al. found increased coupling between the SN and DMN [Sripada et al., 2012]. This discrepancy could perhaps be explained by different methodological approaches and patient samples. Taking all the evidence together, it may be that disequilibrium between these networks is causally associated with PTSD pathophysiology.

In addition, PTSD-related alterations in the nodal centralities were found in the visual cortex (bilateral MOG and left LG). Decreased nodal centrality of left LG has been associated with hypofunction of autobiographical and declarative memory in PTSD patients [Yin et al., 2012]. The increased nodal centralities of the bilateral MOG might be related to flashbacks, which refer to intrusive and involuntary memories; flashbacks in PTSD are known to be associated with increased activation of the middle-occipital cortex [Whalley et al., 2013].

The study had several limitations. First, the nodal centrality results did not survive application of an FDR threshold of $q = 0.05$ to address the multiple-comparison problem perhaps because of our relatively small sample size. This study should, therefore, be considered exploratory. Second, the choice of network nodes has been somewhat arbitrary across published studies. We used the AAL atlas to parcellate the entire brain into 90 regions, but differences in template parcellations might have caused considerable variations in graph-based theoretical parameters, which must be explicitly compared in future work. Third, physiological noise, including respiratory and cardiac fluctuations, might have compromised our results. Fourth, the study lacked a comparison group of subjects who were not exposed to trauma. An earlier study showed altered resting-state functional connectivity in trauma-exposed non-PTSD subjects [Lui et al., 2009]. Fifth, we did not obtain the developmental and pregnancy histories of the subjects or any data concerning possible psychopathology prior to the trauma. Future studies should consider these issues when collecting data. Sixth, we studied only pediatric PTSD patients exposed to an earthquake, which limited the ability to generalize to other types of trauma [Kim et al., 2007]. Seventh, the P value of the positive correlation between the C_p and nodal efficiency of the left SFG and the CAPS score in pediatric PTSD patients was close to 0.05, so this analysis should be considered exploratory. To increase statistical power, future studies must be conducted using a larger sample of PTSD patients; with strict inclusion and criteria such as we have used, this will involve the screening of very large numbers of trauma-exposed subjects.

CONCLUSIONS

The functional connectome of pediatric PTSD patients showed a shift toward a regular configuration, and the disequilibrium among the DMN, SN, and CEN might be associated with PTSD pathophysiology. These topological abnormalities could be potential biomarkers.

REFERENCES

Achard S, Bullmore E (2007): Efficiency and cost of economical brain functional networks. PLoS Comput Biol 3:e17.

Andrews-Hanna JR (2012): The brain's default network and its adaptive role in internal mentation. The. Neuroscientist 18: 251–270.

Bassett DS, Meyer-Lindenberg A, Achard S, Duke T, Bullmore E (2006): Adaptive reconfiguration of fractal small-world human brain functional networks. Proc Natl Acad Sci USA 103:19518–19523.

Benjamini Y, Drai D, Elmer G, Kafkafi N, Golani I (2001): Controlling the false discovery rate in behavior genetics research. Behav Brain Res 125:279–284.

Bernhardt BC, Chen Z, He Y, Evans AC, Bernasconi N (2011): Graph-theoretical analysis reveals disrupted small-world organization of cortical thickness correlation networks in temporal lobe epilepsy. Cereb Cortex 21:2147–2157.

Blake DD, Weathers FW, Nagy LM, Kaloupek DG, Gusman FD, Charney DS, Keane TM (1995): The development of a Clinician-Administered PTSD Scale. J Trauma Stress 8:75–90.

Buckner RL, Andrews-Hanna JR, Schacter DL (2008): The brain's default network: Anatomy, function, and relevance to disease. Ann N Y Acad Sci 1124:1–38.

Bullmore E, Sporns O (2009): Complex brain networks: Graph theoretical analysis of structural and functional systems. Nat Rev Neurosci 10:186–198.

Bullmore ET, Bassett DS (2011): Brain graphs: Graphical models of the human brain connectome. Ann Rev Clin Psychol 7:113–140.

Caeyenberghs K, Leemans A, Heitger MH, Leunissen I, Dhollander T, Sunaert S, Dupont P, Swinnen SP (2012): Graph analysis of functional brain networks for cognitive control of action in traumatic brain injury. Brain 135:1293–1307.

Carrion VG, Garrett A, Menon V, Weems CF, Reiss AL (2008): Posttraumatic stress symptoms and brain function during a response-inhibition task: An fMRI study in youth. Depress Anxiety 25:514−526.

Carrion VG, Weems CF, Watson C, Eliez S, Menon V, Reiss AL (2009): Converging evidence for abnormalities of the prefrontal cortex and evaluation of midsagittal structures in pediatric posttraumatic stress disorder: An MRI study. Psychiatry Res 172:226–234.

Daniels JK, McFarlane AC, Bluhm RL, Moores KA, Clark CR, Shaw ME, Williamson PC, Densmore M, Lanius RA (2010): Switching between executive and default mode networks in posttraumatic stress disorder: Alterations in functional connectivity. J Psychiatry Neurosci 35:258–266.

De Bellis MD, Keshavan MS (2003): Sex differences in brain maturation in maltreatment-related pediatric posttraumatic stress disorder. Neurosci Biobehav Rev 27:103–117.

De Bellis MD, Keshavan MS, Clark DB, Casey BJ, Giedd JN, Boring AM, Frustaci K, Ryan ND (1999): A.E. Bennett Research Award. Developmental traumatology. Part II: Brain development. Biol Psychiatry 45:1271–1284.

De Bellis MD, Keshavan MS, Frustaci K, Shifflett H, Iyengar S, Beers SR, Hall J (2002a): Superior temporal gyrus volumes in maltreated children and adolescents with PTSD. Biol Psychiatry 51:544–552.

De Bellis MD, Keshavan MS, Shifflett H, Iyengar S, Beers SR, Hall J, Moritz G (2002b): Brain structures in pediatric maltreatment-related posttraumatic stress disorder: A sociodemographically matched study. Biol Psychiatry 52:1066–1078.

Dunlop SA, Archer MA, Quinlivan JA, Beazley LD, Newnham JP (1997): Repeated prenatal corticosteroids delay myelination in the ovine central nervous system. J Matern Fetal Med 6:309–313.

Felmingham K, Kemp AH, Williams L, Falconer E, Olivieri G, Peduto A, Bryant R (2008): Dissociative responses to conscious and non-conscious fear impact underlying brain function in post-traumatic stress disorder. Psychol Med 38:1771–1780.

First M, Spitzer R, Gibbon M, Williams J (2002): Structured Clinical Interview for DSM-IV-TR Axis I DSM-IV Disorders, Research Version, Patient Edition (SCID-I/P). New York: Biometrics Research, New York State. Psychiatric Institute.

Fox MD, Zhang D, Snyder AZ, Raichle ME (2009): The global signal and observed anticorrelated resting state brain networks. J Neurophysiol 101:3270–3283.

He Y, Chen Z, Evans A (2008): Structural insights into aberrant topological patterns of large-scale cortical networks in Alzheimer's disease. J Neurosci 28:4756–4766.

He Y, Chen ZJ, Evans AC (2007): Small-world anatomical networks in the human brain revealed by cortical thickness from MRI. Cereb Cortex 17:2407–2419.

Jackowski AP, Douglas-Palumberi H, Jackowski M, Win L, Schultz RT, Staib LW, Krystal JH, Kaufman J (2008): Corpus callosum in maltreated children with posttraumatic stress disorder: A diffusion tensor imaging study. Psychiatry Res 162:256–261.

Jin C, Gao C, Chen C, Ma S, Netra R, Wang Y, Zhang M, Li D (2011): A preliminary study of the dysregulation of the resting networks in first-episode medication-naive adolescent depression. Neurosci Lett 503:105–109.

Jin C, Qi R, Yin Y, Hu X, Duan L, Xu Q, Zhang Z, Zhong Y, Feng B, Xiang H, Gong Q, Liu Y, Lu G, Li L (2014): Abnormalities in whole-brain functional connectivity observed in treatment-naive post-traumatic stress disorder patients following an earthquake. Psychol Med 44:1927–1936.

Joseph D'Ercole A, Ye P (2008): Expanding the mind: Insulin-like growth factor I and brain development. Endocrinology 149: 5958–5962.

Kilpatrick DG, Ruggiero KJ, Acierno R, Saunders BE, Resnick HS, Best CL (2003): Violence and risk of PTSD, major depression, substance abuse/dependence, and comorbidity: Results from the National Survey of Adolescents. J Consult Clin Psychol 71: 692–700.

Kim SJ, Lyoo IK, Lee YS, Kim J, Sim ME, Bae SJ, Kim HJ, Lee JY, Jeong DU (2007): Decreased cerebral blood flow of thalamus in PTSD patients as a strategy to reduce re-experience symptoms. Acta Psychiatr Scand 116:145–153.

Lanius RA, Williamson PC, Densmore M, Boksman K, Neufeld RW, Gati JS, Menon RS (2004): The nature of traumatic memories: A 4-T FMRI functional connectivity analysis. Am J Psychiatry 161:36–44.

Lanius RA, Williamson PC, Hopper J, Densmore M, Boksman K, Gupta MA, Neufeld RW, Gati JS, Menon RS (2003): Recall of emotional states in posttraumatic stress disorder: An fMRI investigation. Biol Psychiatry 53:204–210.

Latora V, Marchiori M (2001): Efficient behavior of small-world networks. Phys Rev Lett 87:198701.

Li Y, Jewells V, Kim M, Chen Y, Moon A, Armao D, Troiani L, Markovic-Plese S, Lin W, Shen D (2013): Diffusion tensor imaging based network analysis detects alterations of neuroconnectivity in patients with clinically early relapsing-remitting multiple sclerosis. Hum Brain Mapp 34:3376–3391.

Liao W, Zhang Z, Pan Z, Mantini D, Ding J, Duan X, Luo C, Lu G, Chen H (2010): Altered functional connectivity and small-world in mesial temporal lobe epilepsy. PloS One 5:e8525.

Liberzon I, Sripada CS (2008): The functional neuroanatomy of PTSD: A critical review. Prog Brain Res 167:151−169.

Lindauer RJ, Booij J, Habraken JB, van Meijel EP, Uylings HB, Olff M, Carlier IV, den Heeten GJ, van Eck-Smit BL, Gersons BP (2008): Effects of psychotherapy on regional cerebral blood flow during trauma imagery in patients with post-traumatic stress disorder: A randomized clinical trial. Psychol Med 38: 543–554.

Liu Y, Liang M, Zhou Y, He Y, Hao Y, Song M, Yu C, Liu H, Liu Z, Jiang T (2008): Disrupted small-world networks in schizophrenia. Brain 131:945–961.

Long Z, Duan X, Xie B, Du H, Li R, Xu Q, Wei L, Zhang SX, Wu Y, Gao Q, Chen H (2013): Altered brain structural connectivity in post-traumatic stress disorder: A diffusion tensor imaging tractography study. J Affect Disord 150:798–806.

Lui S, Huang X, Chen L, Tang H, Zhang T, Li X, Li D, Kuang W, Chan RC, Mechelli A, Sweeney JA, Gong Q (2009): High-field MRI reveals an acute impact on brain function in survivors of the magnitude 8.0 earthquake in China. Proc Natl Acad Sci USA 106:15412–15417.

Lynall ME, Bassett DS, Kerwin R, McKenna PJ, Kitzbichler M, Muller U, Bullmore E (2010): Functional connectivity and brain networks in schizophrenia. J Neurosci 30:9477–9487.

Menon V (2011): Large-scale brain networks and psychopathology: A unifying triple network model. Trends Cogn Sci 15:483–506.

Newman ME (2003): Mixing patterns in networks. Phys Rev E Stat Nonlin Soft Matter Phys 67:026126.

Patel R, Spreng RN, Shin LM, Girard TA (2012): Neurocircuitry models of posttraumatic stress disorder and beyond: A meta-analysis of functional neuroimaging studies. Neurosci Biobehav Rev 36:2130−2142.

Richert KA, Carrion VG, Karchemskiy A, Reiss AL (2006): Regional differences of the prefrontal cortex in pediatric PTSD: An MRI study. Depress Anxiety 23:17–25.

Rose AB, Merke DP, Clasen LS, Rosenthal MA, Wallace GL, Vaituzis AC, Fields JD, Giedd JN (2004): Effects of hormones and sex chromosomes on stress-influenced regions of the developing pediatric brain. Ann N Y Acad Sci 1032:231–233.

Sahara S, O'Leary DD (2009): Fgf10 regulates transition period of cortical stem cell differentiation to radial glia controlling generation of neurons and basal progenitors. Neuron 63:48–62.

Seeley WW, Menon V, Schatzberg AF, Keller J, Glover GH, Kenna H, Reiss AL, Greicius MD (2007): Dissociable intrinsic connectivity networks for salience processing and executive control. J Neurosci 27:2349–2356.

Simantov R, Blinder E, Ratovitski T, Tauber M, Gabbay M, Porat S (1996): Dopamine-induced apoptosis in human neuronal cells: Inhibition by nucleic acids antisense to the dopamine transporter. Neuroscience 74:39–50.

Sporns O, Honey CJ, Kotter R (2007): Identification and classification of hubs in brain networks. PloSOne 2:e1049.

Sporns O, Zwi JD (2004): The small world of the cerebral cortex. Neuroinformatics 2:145–162.

Sridharan D, Levitin DJ, Menon V (2008): A critical role for the right fronto-insular cortex in switching between central-executive and default-mode networks. Proc Natl Acad Sci USA 105:12569–12574.

Sripada RK, King AP, Welsh RC, Garfinkel SN, Wang X, Sripada CS, Liberzon I (2012): Neural dysregulation in posttraumatic stress disorder: Evidence for disrupted equilibrium between salience and default mode brain networks. Psychosom Med 74: 904–911.

Strogatz SH (2001): Exploring complex networks. Nature 410:268–276.

Supekar K, Menon V, Rubin D, Musen M, Greicius MD (2008): Network analysis of intrinsic functional brain connectivity in Alzheimer's disease. PLoS Comput Biol 4:e1000100.

Tanapat P, Galea LA, Gould E (1998): Stress inhibits the proliferation of granule cell precursors in the developing dentate gyrus. Int J Dev Neurosc 16:235–239.

Tao H, Guo S, Ge T, Kendrick KM, Xue Z, Liu Z, Feng J (2013): Depression uncouples brain hate circuit. Mol Psychiatry 18:101–111.

Teicher MH, Dumont NL, Ito Y, Vaituzis C, Giedd JN, Andersen SL (2004): Childhood neglect is associated with reduced corpus callosum area. Biol Psychiatry 56:80–85.

Todd RD (1992): Neural development is regulated by classical neurotransmitters: Dopamine D2 receptor stimulation enhances neurite outgrowth. Biol Psychiatry 31:794–807.

Tzourio-Mazoyer N, Landeau B, Papathanassiou D, Crivello F, Etard O, Delcroix N, Mazoyer B, Joliot M (2002): Automated anatomical labeling of activations in SPM using a macroscopic anatomical parcellation of the MNI MRI single-subject brain. NeuroImage 15:273–289.

Wang J, Wang L, Zang Y, Yang H, Tang H, Gong Q, Chen Z, Zhu C, He Y (2009a): Parcellation-dependent small-world brain functional networks: a resting-state fMRI study. Hum Brain Mapp 30:1511–1523.

Wang L, Zhu C, He Y, Zang Y, Cao Q, Zhang H, Zhong Q, Wang Y (2009b): Altered small-world brain functional networks in children with attention-deficit/hyperactivity disorder. Hum Brain Mapp 30:638–649.

Watts DJ, Strogatz SH (1998): Collective dynamics of 'small-world' networks. Nature 393:440–442.

Weathers FW, Litz BT, Huska JA, Keane TM (1994): PTSD Checklist–Civilian Version, National Center for PTSD. Boston: Behavioral Science Division.

Weber DL, Clark CR, McFarlane AC, Moores KA, Morris P, Egan GF (2005): Abnormal frontal and parietal activity during working memory updating in post-traumatic stress disorder. Psychiatry Res 140:27–44.

Weber M, Killgore WD, Rosso IM, Britton JC, Schwab ZJ, Weiner MR, Simon NM, Pollack MH, Rauch SL (2013): Voxel-based morphometric gray matter correlates of posttraumatic stress disorder. J Anxiety Disord 27:413–419.

Wen W, Zhu W, He Y, Kochan NA, Reppermund S, Slavin MJ, Brodaty H, Crawford J, Xia A, Sachdev P (2011): Discrete neuroanatomical networks are associated with specific cognitive abilities in old age. J Neurosci 31:1204–1212.

Whalley MG, Kroes MC, Huntley Z, Rugg MD, Davis SW, Brewin CR (2013): An fMRI investigation of posttraumatic flashbacks. Brain Cogn 81:151–159.

Whalley MG, Rugg MD, Smith AP, Dolan RJ, Brewin CR (2009): Incidental retrieval of emotional contexts in post-traumatic stress disorder and depression: An fMRI study. Brain Cogn 69: 98–107.

Yang P, Wu MT, Hsu CC, Ker JH (2004): Evidence of early neurobiological alternations in adolescents with posttraumatic stress disorder: A functional MRI study. Neurosci Lett 370: 13–18.

Yin Y, Jin C, Eyler LT, Jin H, Hu X, Duan L, Zheng H, Feng B, Huang X, Shan B, Gong Q, Li L (2012): Altered regional homogeneity in post-traumatic stress disorder: A resting-state functional magnetic resonance imaging study. Neurosci Bull 28:541–549.

Zalesky A, Fornito A, Bullmore ET (2010): Network-based statistic: Identifying differences in brain networks. NeuroImage 53: 1197–1207.

Zalesky A, Fornito A, Seal ML, Cocchi L, Westin CF, Bullmore ET, Egan GF, Pantelis C (2011): Disrupted axonal fiber connectivity in schizophrenia. Biol Psychiatry 69:80–89.

Zhang J, Wang J, Wu Q, Kuang W, Huang X, He Y, Gong Q (2011): Disrupted brain connectivity networks in drug-naive, first-episode major depressive disorder. Biol Psychiatry 70: 334–342.